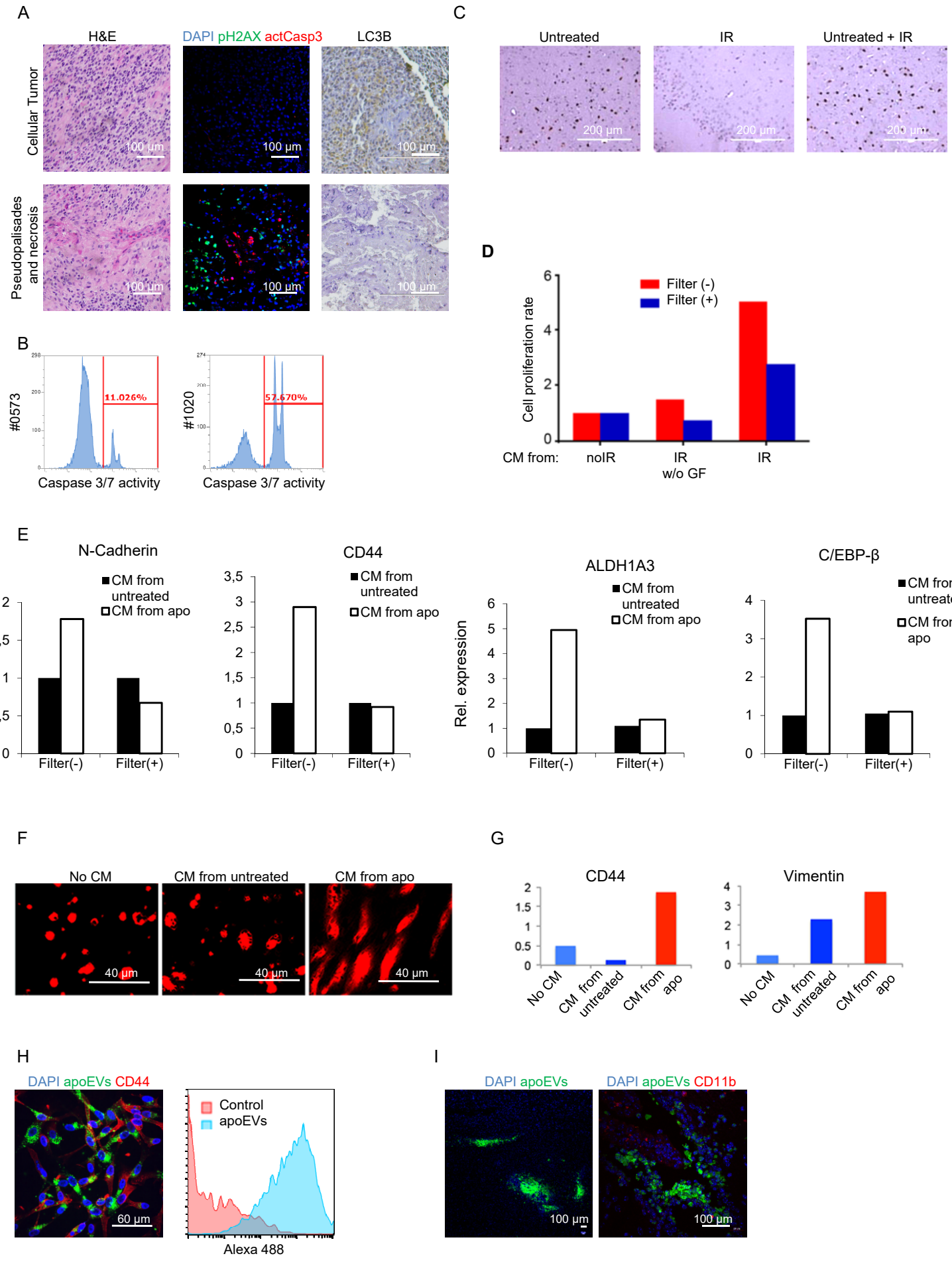
A
H&E
DAPI pH2AX actCasp3
LC3B
Cellular Tumor
Pseudopalisades and necrosis
100 µm
B
#0573
11.026%
Caspase 3/7 activity
#1020
57.670%
Caspase 3/7 activity
C
Untreated
IR
Untreated + IR
200 µm
D
Filter (-)
Filter (+)
Cell proliferation rate
CM from:
noIR
IR w/o GF
IR
E
N-Cadherin
CD44
ALDH1A3
C/EBP-β
CM from untreated
CM from apo
Rel. expression
Filter(-)
Filter(+)
F
No CM
CM from untreated
CM from apo
40 µm
G
CD44
Vimentin
No CM
CM from untreated
CM from apo
H
DAPI apoEVs CD44
60 µm
Control
apoEVs
Alexa 488
I
DAPI apoEVs
DAPI apoEVs CD11b
100 µm

Figure S1 (Related to Figure 1). Apoptotic GBM cells promote more aggressive phenotype of surviving GBM cells

(A) H&E staining of sections obtained from different regions of the same GBM tumor (left panel). Staining of GBM tumor sections with DAPI (blue) antibodies against phospho-H2AX (green) and activated Caspase-3 (red) (middle panel). Immunohistochemical staining of GBM tumor sections with antibodies against LC3B (right panel).

(B) Flow cytometry analysis of caspase 3/7 activity in freshly dissociated GBM tumors from n=5 different patients.

(C) Representative images of mouse brain sections stained for human nuclear antigen after intracranial transplantation of untreated 157 glioma spheres alone, lethally irradiated GBM157 spheres alone, or both together (ratio 1:1). n=5 mice per group.

(D) *In vitro* cell growth assay of GBM157 spheres cultivated for 7 days with conditioned medium from irradiated or non irradiated GBM157 cells. Conditioned medium was either filtered or unfiltered.

(E) qRT-PCR analysis of CD44, ALDH1A3, N-Cadherin and C/EBP-β expression in 157 glioma spheres that were cultivated with either filtered (0.1 μm pore size filter) or unfiltered conditioned medium from GBM157 cells that were either untreated or lethally irradiated and incubated for 4 days prior to medium collection. PCR data were normalized to GAPDH expression level.

(F) Mouse brain sections stained for human Nestin after intracranial transplantation of 157 glioma spheres that were either untreated or pretreated with conditioned medium from irradiated or non-irradiated 157 cells.

(G) Quantification of CD44 and Vimentin expression in brain sections obtained as in “E”.

(H) In vitro uptake of apoEVs into GBM neurospheres. apoEVs were isolated from lethally-irradiated GBM157 neurospheres and labeled with Alexa Fluor 488 5-TFP (green). After extensive washing, labeled apoEVs were added into culture medium of GBM157 spheres. At 16 hr, GBM neurospheres were observed under the confocal microscope (left panel) and analyzed by FACS (right pannel).

(I) In vivo uptake of apoEVs into GBM cells. apoEVs were labeled as in “G” (green) and injected into intracranial tumor that was formed by GBM374 neurospheres. At 16 hr post-injection, mice were sacrificed and brain sections were stained with antibodies against CD11b (red) and observed under the confocal microscope. Left image – low magnification, right image – high magnification stained with antibodies against CD11b. Injection site is indicated with arrow.

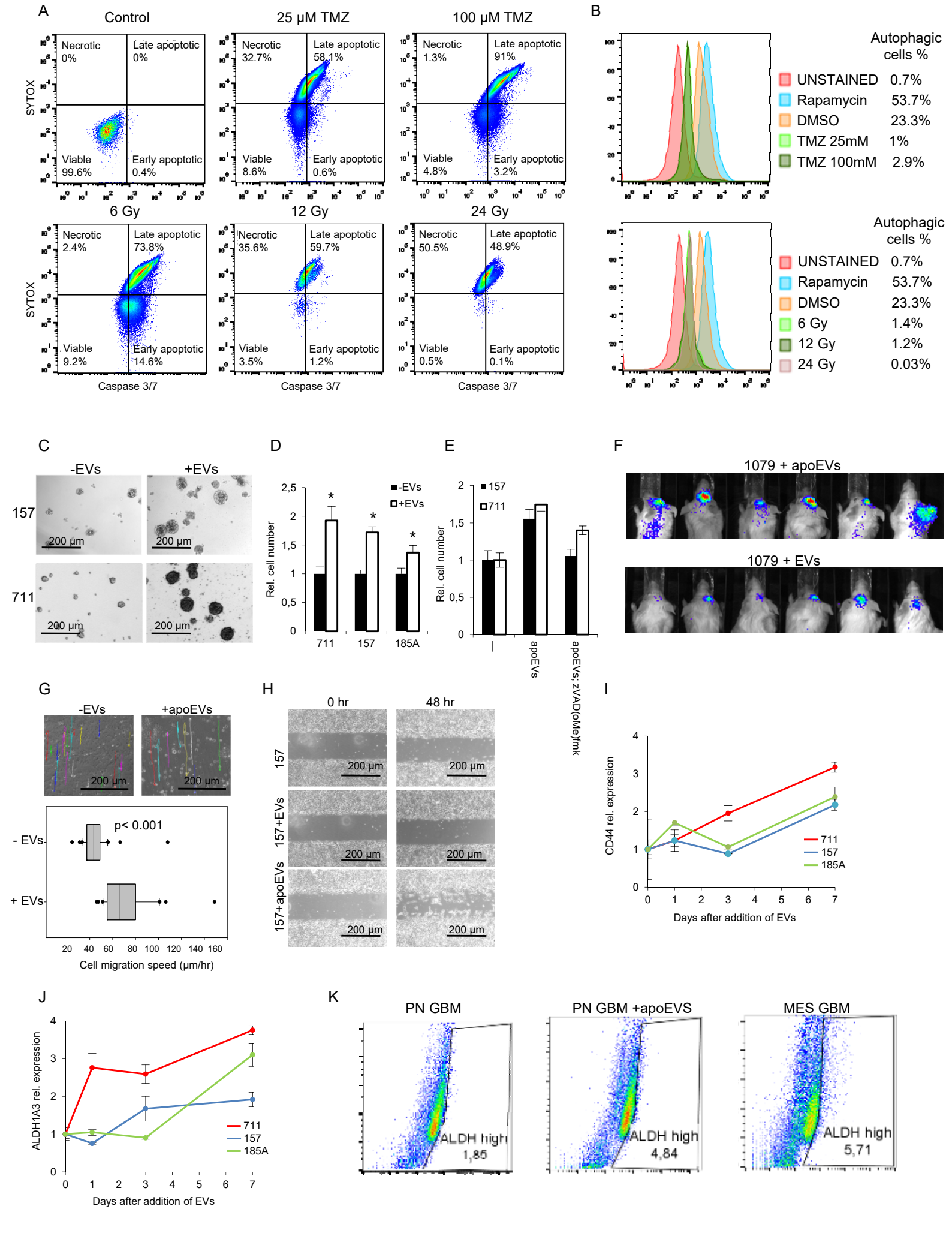
A
Control
25 μM TMZ
100 μM TMZ
Necrotic 0%
Late apoptotic 0%
Viable 99.6%
Early apoptotic 0.4%
Necrotic 32.7%
Late apoptotic 58.1%
Viable 8.6%
Early apoptotic 0.6%
Necrotic 1.3%
Late apoptotic 91%
Viable 4.8%
Early apoptotic 3.2%
SYTOX
6 Gy
12 Gy
24 Gy
Necrotic 2.4%
Late apoptotic 73.8%
Viable 9.2%
Early apoptotic 14.6%
Necrotic 35.6%
Late apoptotic 59.7%
Viable 3.5%
Early apoptotic 1.2%
Necrotic 50.5%
Late apoptotic 48.9%
Viable 0.5%
Early apoptotic 0.1%
Caspase 3/7
B
Autophagic cells %
UNSTAINED 0.7%
Rapamycin 53.7%
DMSO 23.3%
TMZ 25mM 1%
TMZ 100mM 2.9%
Autophagic cells %
UNSTAINED 0.7%
Rapamycin 53.7%
DMSO 23.3%
6 Gy 1.4%
12 Gy 1.2%
24 Gy 0.03%
C
-EVs
+EVs
157
711
200 μm
D
-EVs
+EVs
Rel. cell number
711
157
185A
E
157
711
Rel. cell number
apoEVs
apoEVs; zVAD(oMe)fmk
F
1079 + apoEVs
1079 + EVs
G
-EVs
+apoEVs
200 μm
p< 0.001
- EVs
+ EVs
Cell migration speed (μm/hr)
H
0 hr
48 hr
157
157+EVs
157+apoEVs
200 μm
I
CD44 rel. expression
711
157
185A
Days after addition of EVs
J
ALDH1A3 rel. expression
711
157
185A
Days after addition of EVs
K
PN GBM
PN GBM +apoEVS
MES GBM
ALDH high 1,85
ALDH high 4,84
ALDH high 5,71

Figure S2 (Related to Figures 1 and 2). apoEVs promote a more aggressive phenotype of GBM cells

(A) Flow cytometry analysis of caspase 3/7 activity and SYTOX staining of GBM157 neurospheres treated with different doses of irradiation or temozolomide for 4 days.

(B) Flow cytometry analysis of autophagy in the samples as in "A". Levels of necrosis, apoptosis and autophagy are indicated. Cells treated with rapamycin for 24 hr were used as a positive control to detect autophagy.

(C) Representative Images of GBM157 and GBM711 glioma spheres cultivated for 4 days with or without apoEVs from corresponding cell line.

(D) Cell counting with Countess II (Thermo scientific) of GBM157, GBM711 or GBM0185 spheres cultivated for 7 days with or without apoEVs obtained from corresponding cell lines.

(E) *In vitro* cell growth assay of GBM157 and GBM711 spheres cultivated for 7 days with EVs from corresponding cell lines. EVs donor cells were either untreated, or lethally irradiated and incubated for 4 days in the presence or absence of 20 μM pan-caspase inhibitor zVAD(OMe)fmk.

(F) Representative bioluminescence images of mice intracranially injected with $2 \cdot 10^5$ luciferase labeled GBM1079 neurospheres in the presence of apoEVs produced by lethally irradiated neurospheres from the same patient (apoEVs) or by untreated neurospheres from the same patient (control EVs).

(G) Upper panel- Representative track pattern of individual GBM157 cells that were either untreated or cultivated with apoEVs for 4 days prior to assay. Lower panel- Clonal motility assay of untreated GBM0185 cells and GBM0185 cells that were cultivated with apoEVs for 4 days prior to assay. n=50 cells from two independent experiments. The line in the box is the median, the left and right of the box are the first and third quartiles, and the whiskers extend to 10th and 90th percentiles respectively.

(H) Wound healing assay with untreated GBM157 cells and GBM157 cells that were cultivated with apoEVs or control EVs for 4 days prior to assay.

(I) qRT-PCR analysis of CD44 expression in GBM157, GBM711 and GBM0185 glioma spheres at different time points of cultivation with apoEVs from corresponding cell line. PCR data were normalized to GAPDH expression level.

(J) qRT-PCR analysis of ALDH1A3 expression in GBM157, GBM711 and GBM0185 glioma spheres at different time points of cultivation with apoEVs from corresponding cell line. PCR data were normalized to GAPDH expression level.

(K) FACS analysis with ALDEFLUOR staining of control GBM157 spheres (PN) and spheres that were cultivated with apoEVs for 4 days. 267 spheres (MES) were used as a positive control.

All quantitative data are average ± SD; *$p < 0.01$.

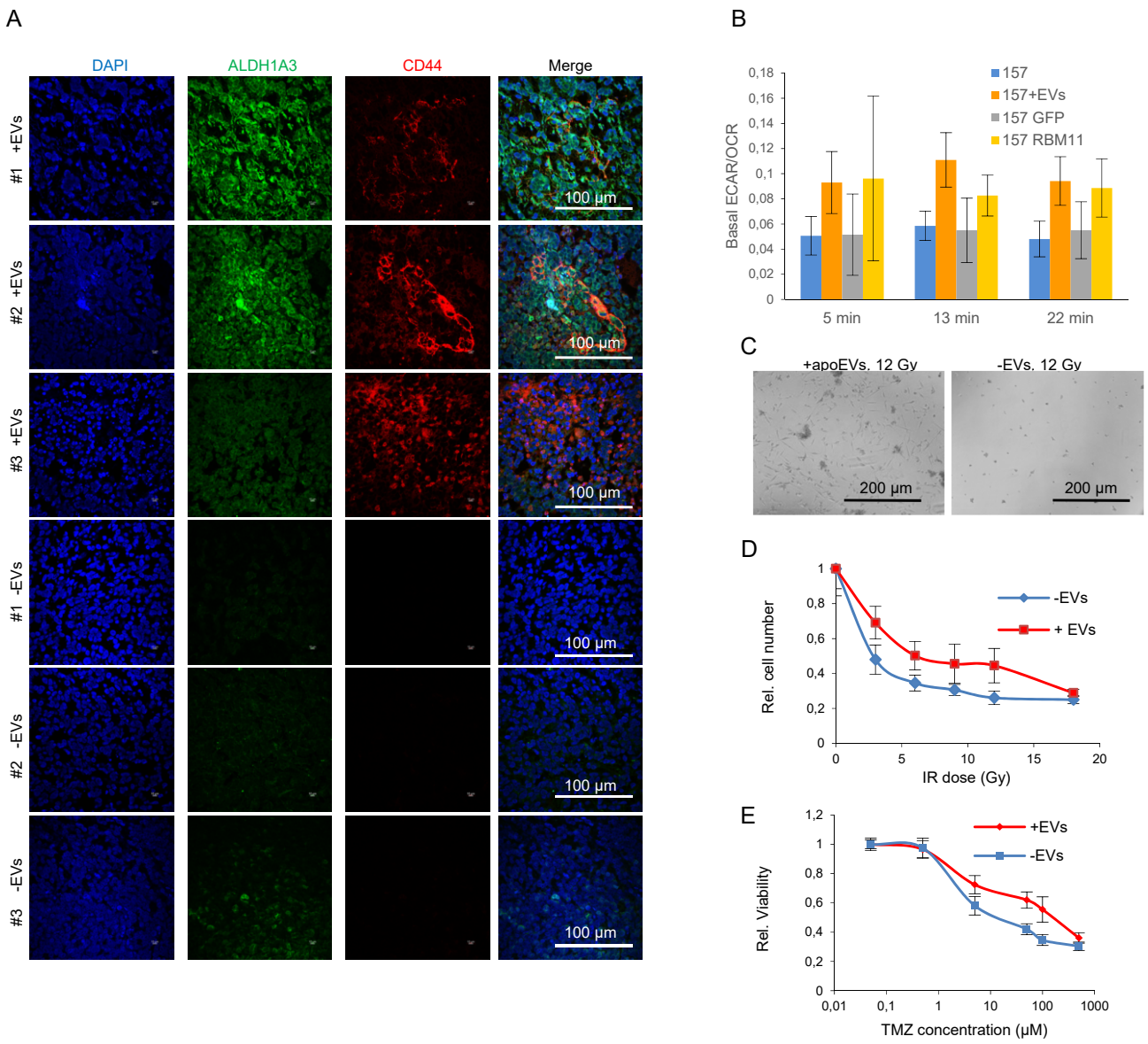
A
DAPI
ALDH1A3
CD44
Merge
#1 +EVs
#2 +EVs
#3 +EVs
#1 -EVs
#2 -EVs
#3 -EVs
100 µm
B
Basal ECAR/OCR
157
157+EVs
157 GFP
157 RBM11
5 min
13 min
22 min
C
+apoEVs, 12 Gy
-EVs, 12 Gy
200 µm
D
Rel. cell number
-EVs
+ EVs
IR dose (Gy)
E
Rel. Viability
+EVs
-EVs
TMZ concentration (µM)
F
EVs from IR
EVs from nonIR
Rel. cell number
EVs concentration (µg/ml)
G
apoEVs
EVs
Rel. cell number
1-2 days
3-4 days
5-6 days
7-8 days
H
HBEC
GBM
Rel. cell number
no EVs
0 Gy
6 Gy
12 Gy
24 Gy
25 µM TMZ
100 µM TMZ
I
apoEVs
EVs
Rel. cell number
no EVs
APO
MVs
EXO
J
apoEVs
EVs
Rel. cell number
no EVs
APO
MVs
EXO
K
Rel. cell number
no EVs
CD63-
CD63+

Figure S3 (Related to Figure 2). apoEVs increase expression of MES markers *in vivo* and therapy resistance *in vitro*

(A) Images of mouse brain sections obtained after intracranial transplantation of 711 glioma spheres alone or together with apoEVs and stained for DNA (blue), ALDH1A3 (green), and CD44 (red).

(B) Ratio of basal extracellular acidification rate (ECAR) and oxygen consumption rate (OCR) measured by a Seahorse Bioanalyzer in GBM157 neurospheres that were either untreated or pretreated with apoEVs for 4 days and in GBM157 neurospheres stably expressing GFP or GFP-RBM11.

(C) Representative images of 157 glioma cells that were either untreated or cultivated with apoEVs for 3 days, followed by irradiation at 12 Gy and incubated for 7 days. In apoEVs treated samples remain the substantial number of viable cells, while in untreated sample, irradiation eliminated nearly all cells.

(D, E) *In vitro* cell viability assay of 711 glioma spheres cultivated with or without apoEVs for 3 days, followed by treatment with various concentrations of temozolomide (TMZ) or different doses of irradiation for 7 days.

(F) *In vitro* cell viability assay of 157 glioma spheres cultivated with various concentrations apoEVs or control EVs for 3 days, followed by treatment with of 5 μM of TMZ for 7 days.

(G) *In vitro* cell growth assay of GBM157 neurospheres cultivated for 7 days with EVs secreted by GBM157 neurospheres for indicated periods of time after 6Gy irradiation (apoEVs) or by untreated GBM157 neurospheres (control EVs).

(H) *In vitro* cell growth assay of GBM157 neurospheres cultivated for 7 days with apoEVs produced by GBM157 neurospheres or human brain endothelial cells (HBEC) that were untreated or treated with 6 Gy, 12 Gy, 24 Gy doses of irradiation or with 25 μM or 100 μM of temozolomide.

(I) *In vitro* cell growth assay of GBM157 spheres cultivated for 7 days with apoEVs or control EVs isolated by centrifugation at 2 000g (apoptotic body: APO), 16 000g (microvesicles: MVs) and 120 000g (exosomes: EXO).

(J) *In vitro* cell viability assay of GBM157 neurospheres cultivated with or without different fractions of apoEVs or control EVs for 3 days, followed by 3 Gy irradiation.

(K) In vitro cell growth assay of GBM157 spheres cultivated for 7 days with $CD63^+$ and $CD63^-$ fractions of apoEVs.

All quantitative data are average ± SD; *$p < 0.01$.

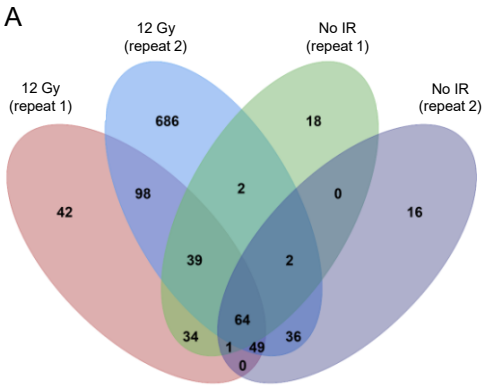

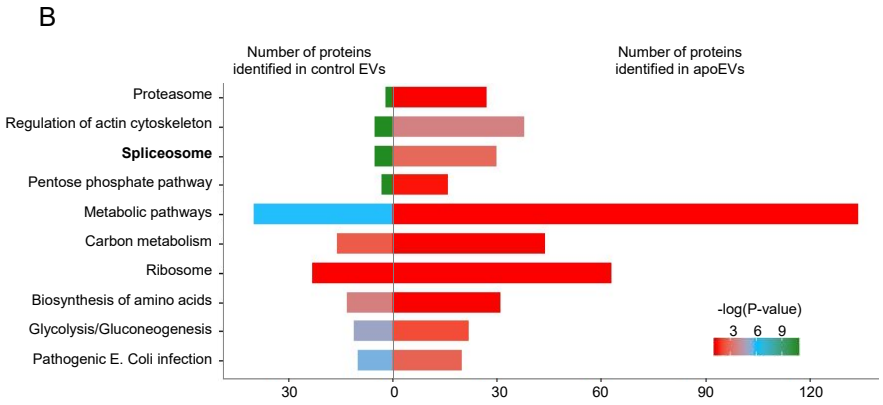

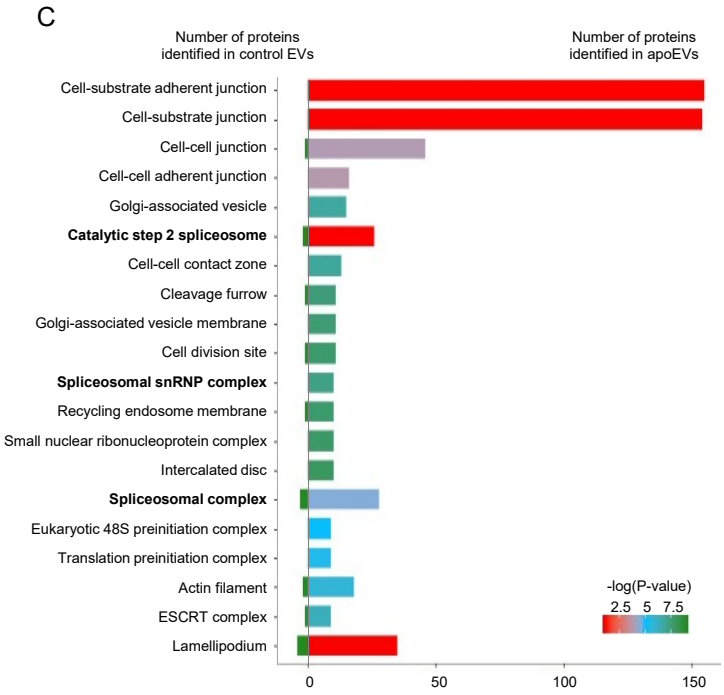

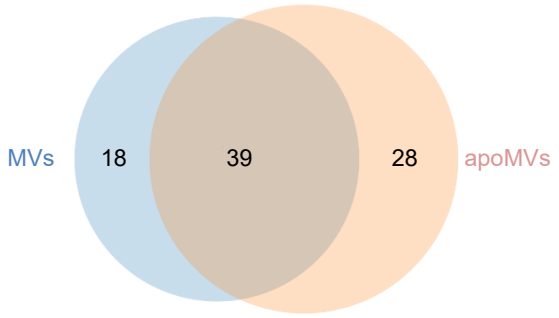

Biological Process (GO)	Gene count	FDR
Protein folding	7	0.00013
Response to organic substance	14	0.00354
Regulation of biological quality	14	0.0242
Response to endoplasmic reticulum stress	5	0.0261
Response to chemical	15	0.0342

KEGG Pathways	Gene count	FDR
Protein processing in endoplasmic reticulum	7	6.63e-07
Thyroid hormone synthesis	4	0.0004

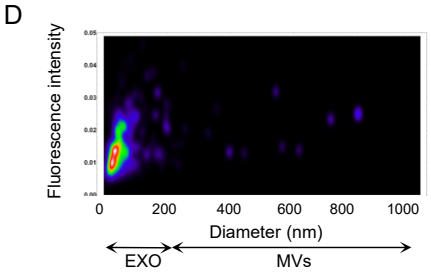

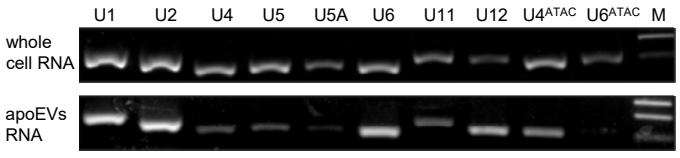

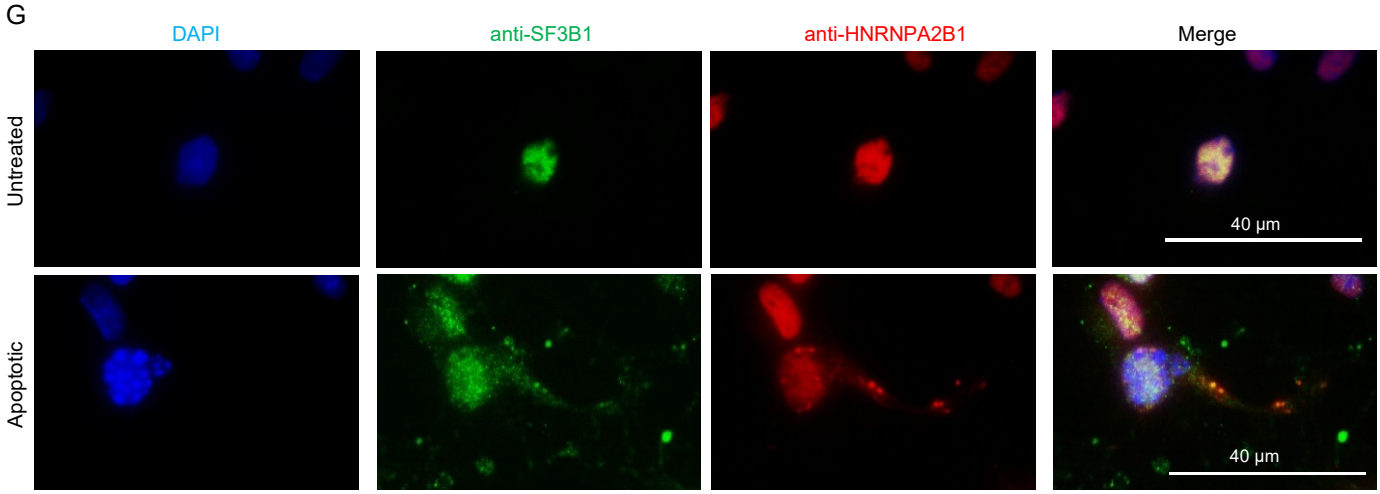

Figure S4 (Related to Figures 3 and 4). apoEVs are enriched with spliceosomal proteins and U snRNAs

(A) Distribution of proteins identified in apoEVs and control EVs during biological and technical replicates of LC-MS/MS experiment.

(B and C) Analysis of proteins identified by LC-MS/MS in apoEVs and control EVs with KEGG database (B) or GO Cellular Component database (C).

(D) Fluorescent NTA analysis of apoEVs produced by GBM157 spheres. Vesicles were stained with Alexa 555 labeled anti-U2AF2 antibodies.

(E) Venn diagram representing the distribution of proteins in microvesicles produced by apoptotic (apoMVs) and untreated (MVs) 157GBM cells. (upper panel) Analysis of proteins identified by LC-MS/MS in apoMVs and control MVs with GO Biological Process and KEGG databases (lower panel).

(F) RT-PCR analysis of different U snRNAs purified from either apoEVs or parental cells.

(G) Immunofluorescent staining of GBM157 neurospheres after induction of apoptosis with 50 µM of cisplatin. Cells were stained with DAPI (blue), anti-SF3B1 (green) and anti-HNRNPA2B1 (red) antibodies.

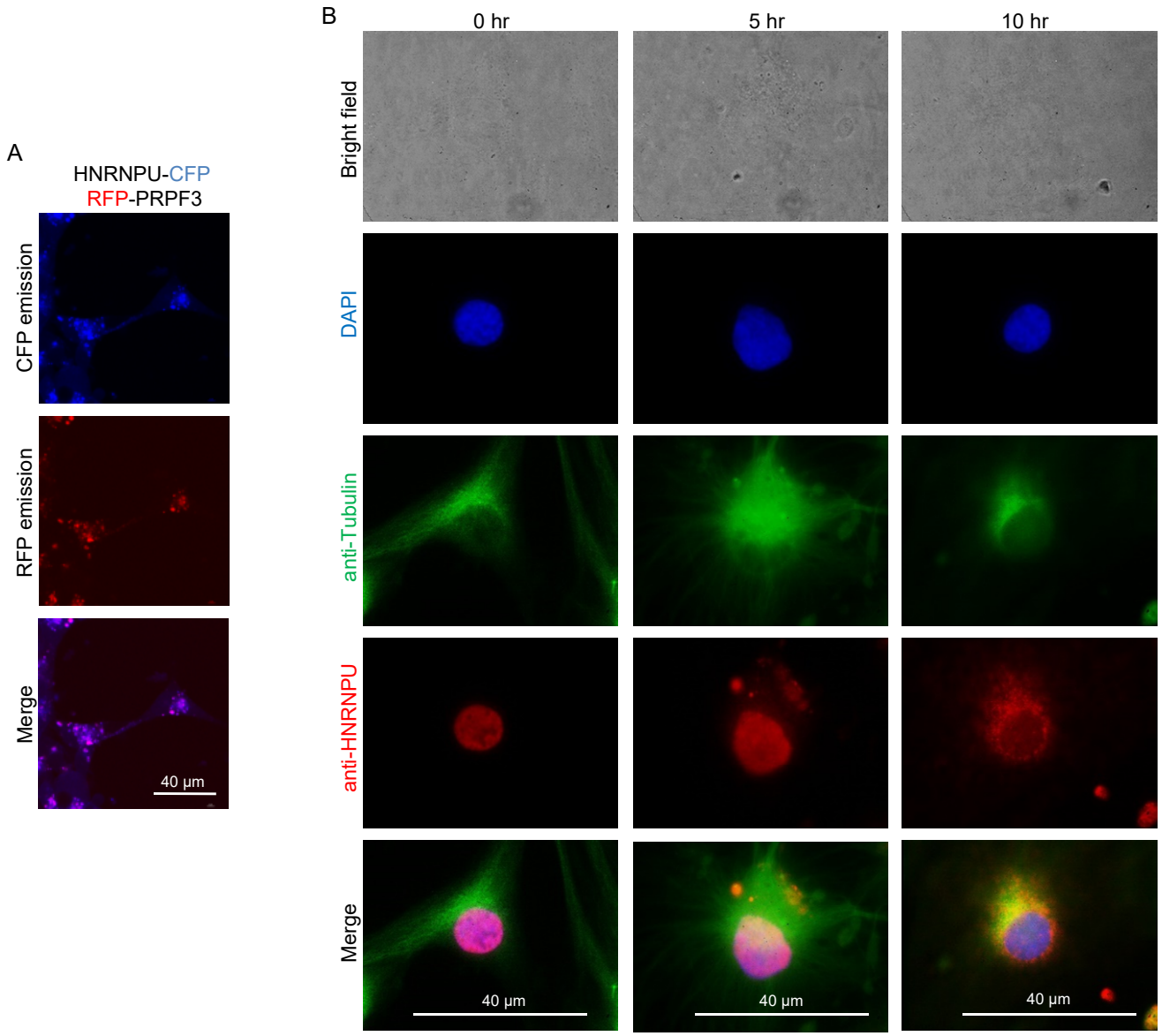
A
HNRNPU-CFP
RFP-PRPF3
CFP emission
RFP emission
Merge
40 μm
B
0 hr
5 hr
10 hr
Bright field
DAPI
anti-Tubulin
anti-HNRNPU
Merge
40 μm
40 μm
40 μm

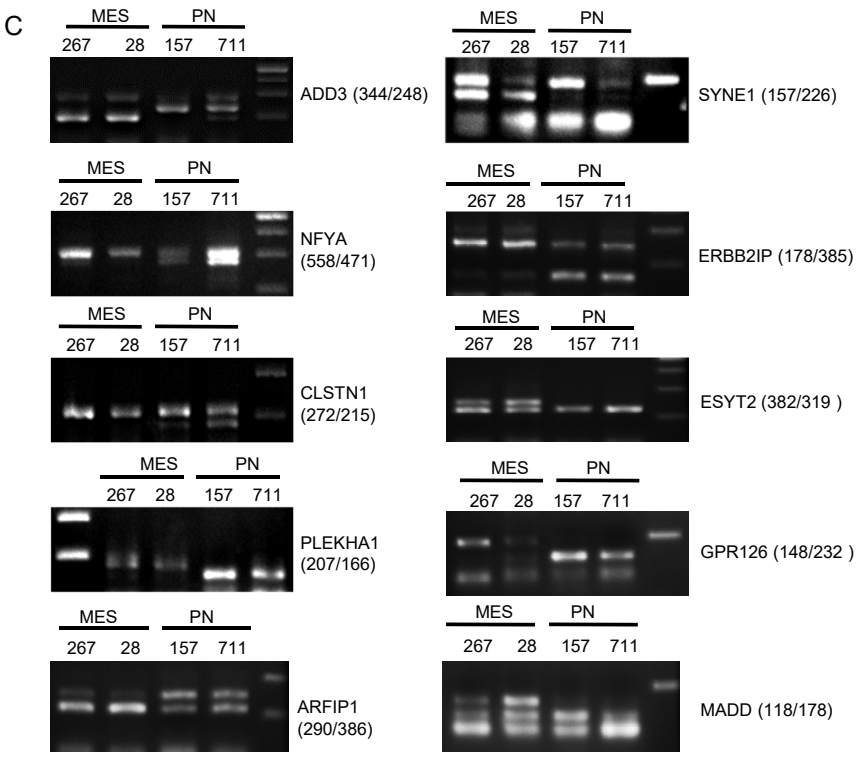
C
MES
PN
267
28
157
711
ADD3 (344/248)
NFYA (558/471)
CLSTN1 (272/215)
PLEKHA1 (207/166)
ARFIP1 (290/386)
SYNE1 (157/226)
ERBB2IP (178/385)
ESYT2 (382/319)
GPR126 (148/232)
MADD (118/178)

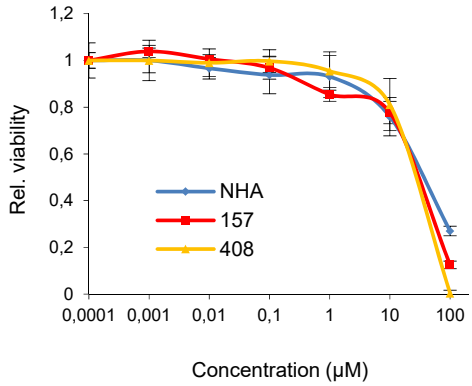
D
Rel. viability
1,2
1
0,8
0,6
0,4
0,2
0
0,0001
0,001
0,01
0,1
1
10
100
NHA
157
408
Concentration (μM)

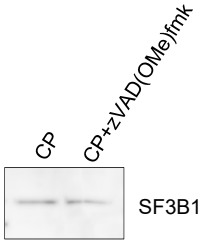
E
CP
CP+zVAD(OMe)fmk
SF3B1

Figure S5 (Related to Figures 4 and 5). Spliceosomal proteins are exported from apoptotic cells in a caspase-dependent manner and induce splicing changes in recipient cells

(A) Fluorescence images of GBM157 cells co-transfected with pTagRFP-PRPF3 (red) and pEYFP-HNRNPU-CFP (blue) plasmids. At 24 hr after transfection, cells were treated with 50 μM of cisplatin (CP) for 10 hr and observed under confocal microscope.

(B) Immunofluorescent staining of GBM157 neurospheres at different time points after induction of apoptosis with 50 μM of cisplatin. Cells were stained with DAPI (blue), anti-aTubulin antibody (green) and anti-C terminal region of HNRNPU antibody (red).

(C) Validation of the RNA-sequencing data by RT-PCR analysis for splicing of different mRNAs identified from two MES (267 and 28) and two PN (157, 711) sphere samples. Lengths of alternative splicing products are indicated.

(D) In vitro viability assay of GBM spheres from two different patients and normal human astrocytes (NHA) treated with Isoginkgetin.

(E) Western blotting analysis of SF3B1 in GBM157 neurospheres treated with cisplatin (CP) in the presence or absence of zVAD(OMe)fmk.

All quantitative data are average ± SD.

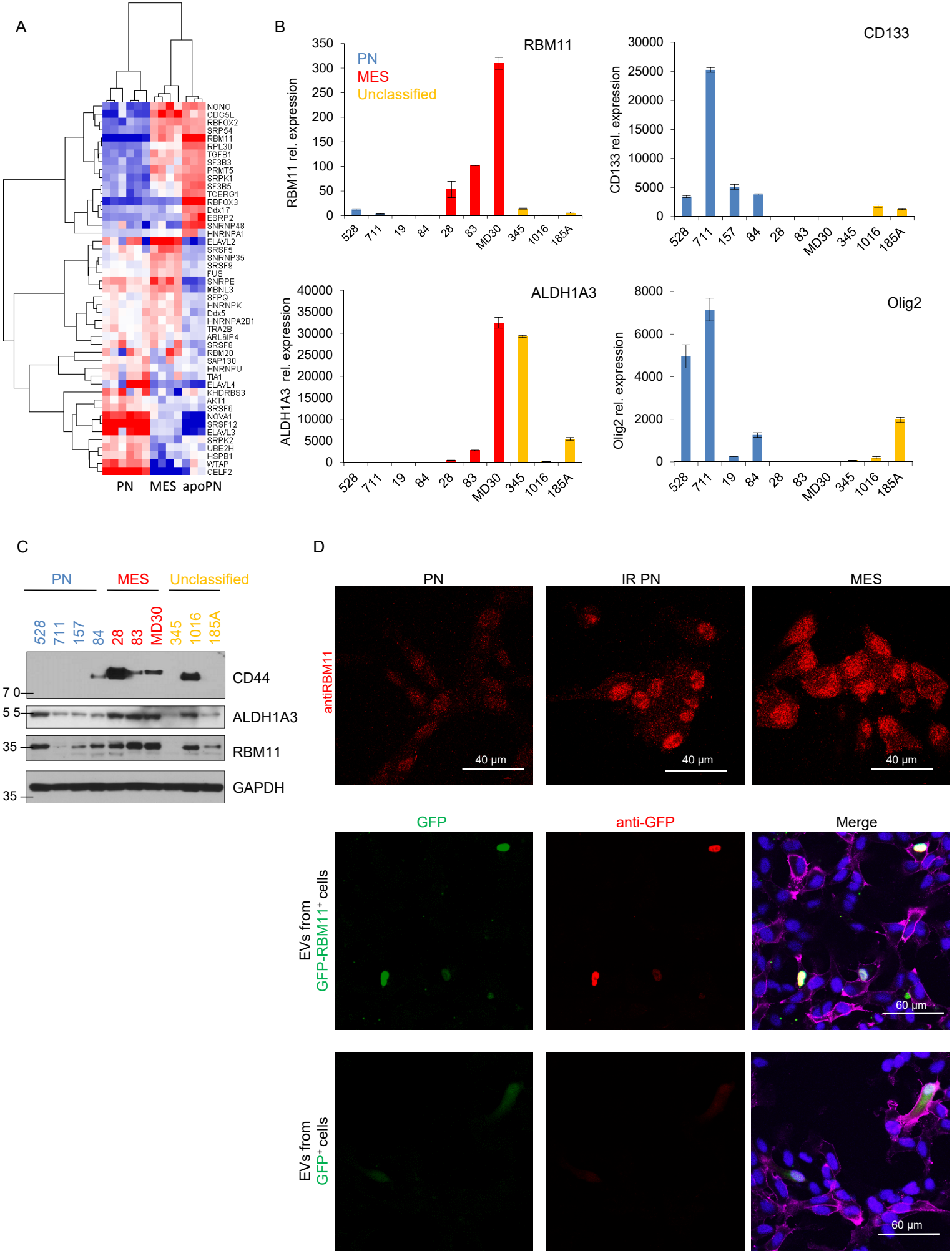
A
NONO
CDC5L
RBFOX2
SRP54
RBM11
RPL30
TGFB1
SF3B3
PRMT5
SRPK1
SF3B5
TCERG1
RBFOX3
Ddx17
ESRP2
SNRNP48
HNRNPA1
ELAVL2
SRSF5
SNRNP35
SRSF9
FUS
SNRPE
MBNL3
SFPQ
HNRNPK
Ddx5
HNRNPA2B1
TRA2B
ARL6IP4
SRSF8
RBM20
SAP130
HNRNPU
TIA1
ELAVL4
KHDRBS3
AKT1
SRSF6
NOVA1
SRSF12
ELAVL3
SRPK2
UBE2H
HSPB1
WTAP
CELF2
PN MES apoPN
B
RBM11
PN
MES
Unclassified
RBM11 rel. expression
CD133
CD133 rel. expression
ALDH1A3
ALDH1A3 rel. expression
Olig2
Olig2 rel. expression
528 711 19 84 28 83 MD30 345 1016 185A
528 711 157 84 28 83 MD30 345 1016 185A
C
PN MES Unclassified
528 711 157 84 28 83 MD30 345 1016 185A
CD44
ALDH1A3
RBM11
GAPDH
70
55
35
35
D
PN
IR PN
MES
antiRBM11
40 µm
GFP
anti-GFP
Merge
EVs from GFP-RBM11+ cells
60 µm
EVs from GFP+ cells
60 µm

Figure S6 (Related to Figure 6). RBM11 is mesenchymal specific splicing factor

(A) Heatmap generated from microarray data showing expression of splicing factor encoding genes in proneural (PN), lethally irradiated proneural (apoPN) and mesenchymal (MES) glioma spheres.

(B) qRT-PCR analysis of ALDH1A3, RBM11, CD133 and Olig2 expression in different glioma sphere lines. PCR data were normalized to GAPDH expression level.

(C) Western blotting analysis of different glioma sphere lines.

(D) Higher resolution images corresponding to panels 6B and 6C.

All quantitative data are average ± SD; *$p < 0.01$.

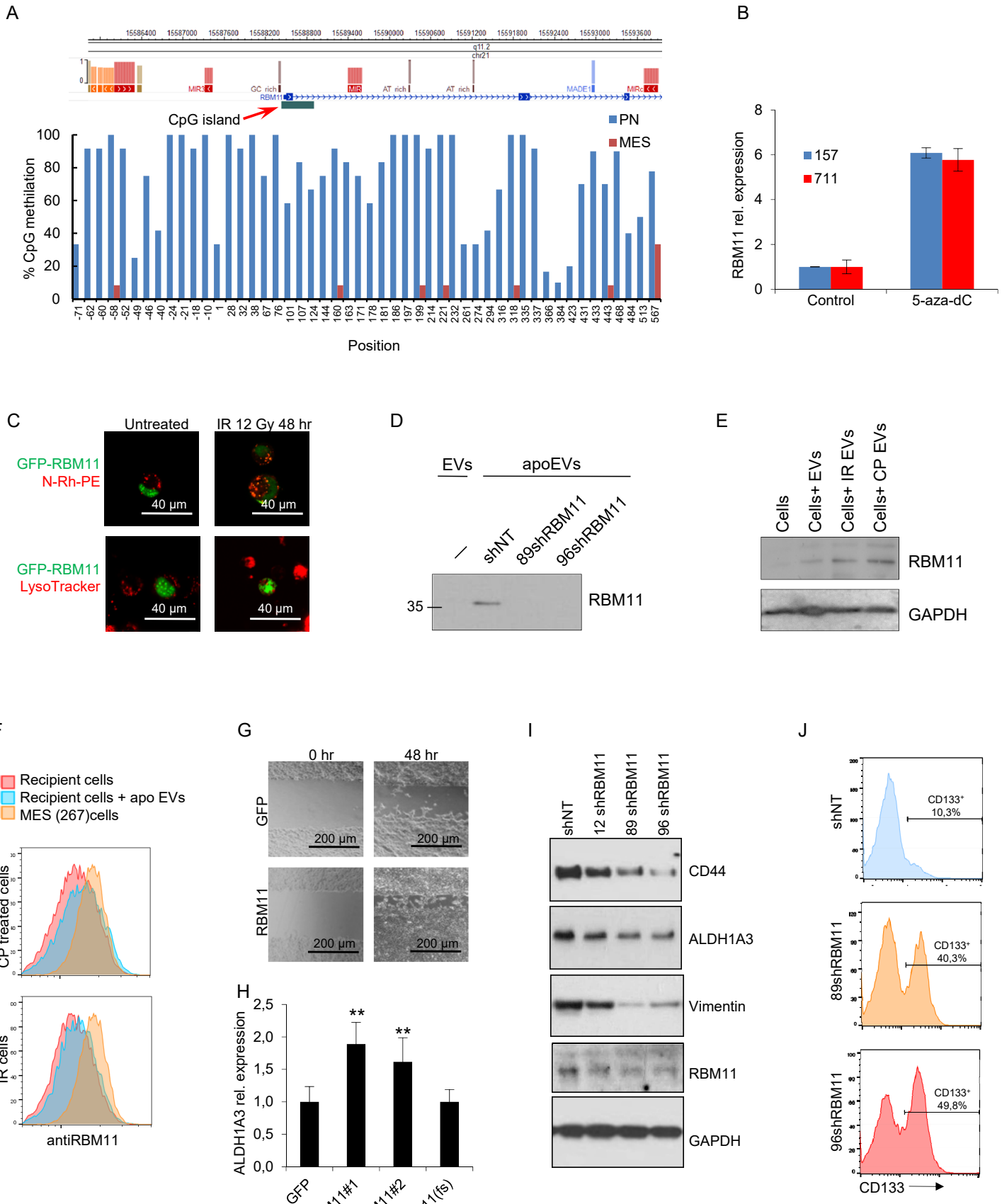
A
CpG island
PN
MES
% CpG methilation
Position
B
RBM11 rel. expression
157
711
Control
5-aza-dC
C
Untreated
IR 12 Gy 48 hr
GFP-RBM11
N-Rh-PE
GFP-RBM11
LysoTracker
40 µm
D
EVs
apoEVs
shNT
89shRBM11
96shRBM11
35
RBM11
E
Cells
Cells+ EVs
Cells+ IR EVs
Cells+ CP EVs
RBM11
GAPDH
F
Recipient cells
Recipient cells + apo EVs
MES (267)cells
apoEVs from CP treated cells
apoEVs from IR cells
antiRBM11
G
0 hr
48 hr
GFP
RBM11
200 µm
H
ALDH1A3 rel. expression
**
GFP
RBM11#1
RBM11#2
RBM11(fs)
I
shNT
12 shRBM11
89 shRBM11
96 shRBM11
CD44
ALDH1A3
Vimentin
RBM11
GAPDH
J
shNT
CD133+ 10,3%
89shRBM11
CD133+ 40,3%
96shRBM11
CD133+ 49,8%
CD133

Figure S7 (Related to Figure 6). Analysis of RBM11 promoter methylation and identification of RBM11 functions in GBM cells

(A) Schematic representation of the CpG island within the RBM11 promoter region (upper panel) and histogram representing methylation levels of individual CpG dinucleotides within the RBM11 promoter in PN and MES glioma spheres (lower panel). Note that the CpG island in PN glioma spheres is largely hypermethylated, whereas that in MES cells is not.

(B) qRT-PCR analysis of RBM11 expression in GBM157 and GBM711 spheres (both PN) incubated for 4 days in the presence or absence of 5 μM of 5-Aza-2′-deoxycytidine – cytosine methylation inhibitor. Obtained data demonstrate increase in RBM11 expression upon inhibition of CpG methylation in PN glioma spheres. PCR data were normalized to GAPDH expression level.

(C) Fluorescence images of GBM157 cells transfected with pTagGFP2-RBM11 plasmid (green). At 24 h after transfection, cells were treated with 50 μM cisplatin (CP) for 10 hr, stained for microvesicular bodies with N-Rh-PE (upper panel) or for lysosomes with LysoTracker Deep Red (lower panel), and observed under confocal microscope. Obtained images demonstrate colocalization of RBM11 with microvesicular bodies but not with lysosomes, indicating that RBM11 undergoes export rather than lysosomal degradation in apoptotic cells (Fader et al., 2008). Similar results were obtained with 1 μM of staurosporine treatment for 10 hr and 4 days after lethal irradiation.

(D) Western blotting analysis of control EVs or apoEVs purified from lethally-irradiated GBM157 cells, stably expressing shRNA against RBM11 or non target (NT) shRNA as a control.

(E) Western blotting analysis of GBM157 neurospheres incubated with EVs from untreated cells and apoEVs purified from lethally irradiated or CP treated cells for 16 hr, untreated cells were used as a control.

(F) FACS analysis for RBM11 staining of control GBM711 spheres or GBM711 spheres incubated for 10 hr with apoEVs from either lethally irradiated or 50 μM cisplatin treated GBM711 cells. 267 spheres (MES) were used as a positive control.

(G) Wound healing assay with GBM157 cells stably expressing either GFP or GFP-RBM11 protein.

(H) qRT-PCR of ALDH1A3 expression in GBM157 cells stably expressing GFP, GFP-RBM11 (two RBM11 isoforms) or GFP-RBM11 frame-shift mutant (fs).

(I) Western blotting analysis of 267 (MES) cells expressing non-target shRNA, or shRNA against RBM11.

(J) FACS analysis for CD133 staining of MES cells expressing non-target shRNA, or shRNA against RBM11.

All quantitative data are average ± SD; $^{**}p < 0.05$.

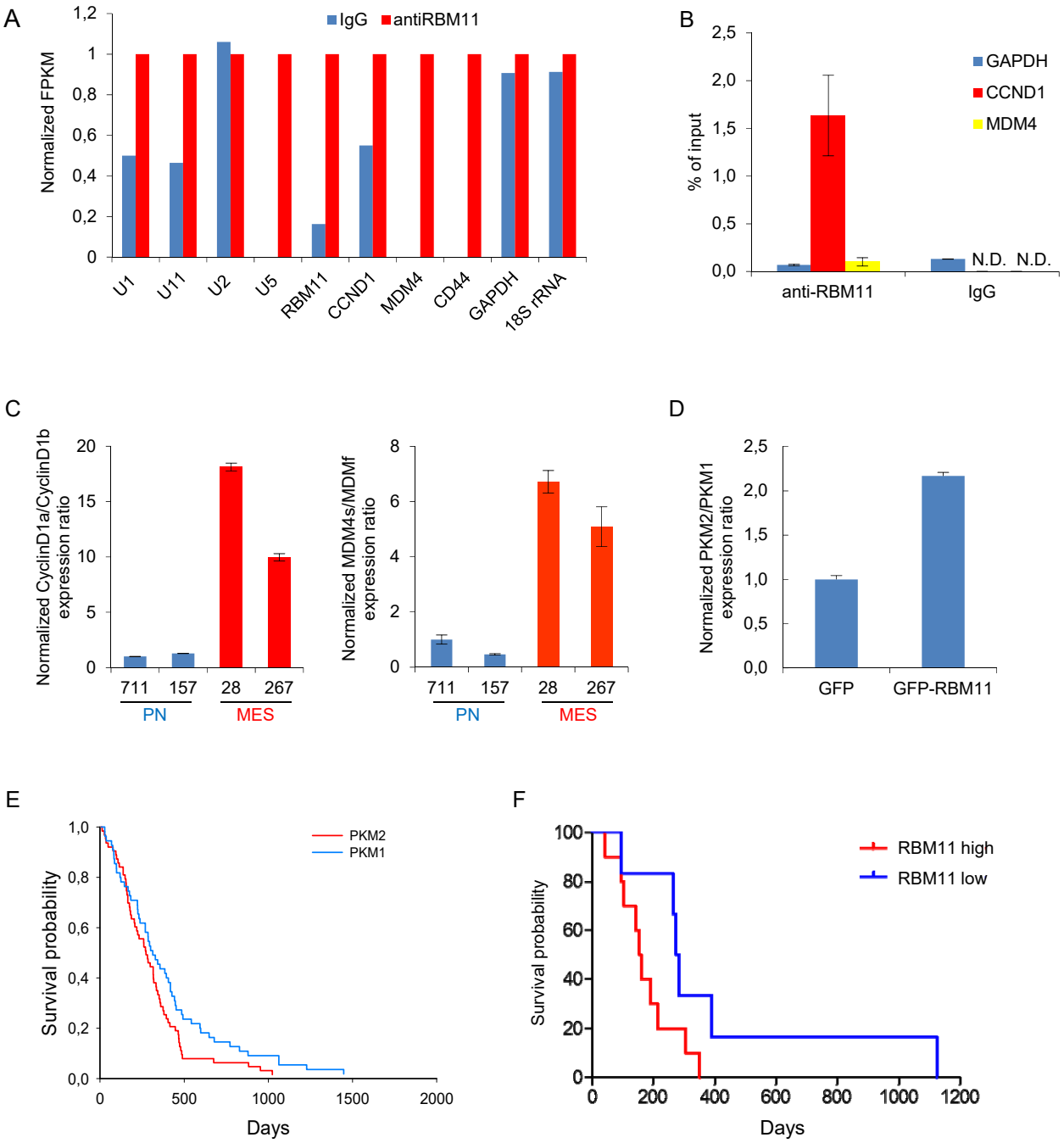
A
IgG
antiRBM11
Normalized FPKM
1,2
1
0,8
0,6
0,4
0,2
0
U1
U11
U2
U5
RBM11
CCND1
MDM4
CD44
GAPDH
18S rRNA
B
GAPDH
CCND1
MDM4
% of input
2,5
2,0
1,5
1,0
0,5
0,0
N.D.
N.D.
anti-RBM11
IgG
C
Normalized CyclinD1a/CyclinD1b expression ratio
20
15
10
5
0
711
157
28
267
PN
MES
Normalized MDM4s/MDMf expression ratio
8
6
4
2
0
711
157
28
267
PN
MES
D
Normalized PKM2/PKM1 expression ratio
2,5
2,0
1,5
1,0
0,5
0,0
GFP
GFP-RBM11
E
PKM2
PKM1
Survival probability
1,0
0,8
0,6
0,4
0,2
0,0
0
500
1000
1500
2000
Days
F
RBM11 high
RBM11 low
Survival probability
100
80
60
40
20
0
0
200
400
600
800
1000
1200
Days

Figure S8 (Related to Figures 7 and 8). Exogenous RBM11 promotes malignancy of recipient tumor cells

(A) RNA immunoprecipitaion and subsequent RNA-sequencing performed with antibodies against RBM11 or a control IgG. Data demonstrates relative enrichment of U1, U11, U5 snRNAs and RBM11, CyclinD1, MDM4 mRNAs in RBM11 precipitated sample. 18S rRNA and GAPDH mRNA are shown as a control.

(B) Validation of the RNA-IP RNA-sequencing data by qRT-PCR analysis with primers for GAPDH, CyclinD1 and MDM4 (N.D. – not detected).

(C) qRT-PCR analysis of CyclinD1 and MDM4 isoform expression ratios in different glioma sphere lines.

(D) qRT-PCR analysis of PKM isoform expression ratios in GBM157 neurospheres (PN subtype) expressing GFP or GFP-RBM11.

(E) Kaplan-Meier curve showing the overall survival of glioma patients subdivided based on the splicing of PKM ($p=0.0494$, log-rank test). RNAseq data were obtained from TCGA database.

(F) Kaplan-Meier curve showing the overall survival of glioma patients ($n=16$) subdivided based on RBM11 immunoreactivity ($p=0.0767$, log-rank test), data obtained from the tissue microarray.

All quantitative data are average ± SD; $*p < 0.01$.